Autonomous oscillations in Saccharomyces cerevisiae during batch cultures on trehalose

Matthieu Jules, Jean Marie François, Jean-Luc Parrou

Autonomous oscillations in *Saccharomyces cerevisiae* during batch cultures on trehalose

Matthieu Jules, Jean François and Jean Luc Parrou

Centre de Bioingenierie Gilbert Durand, UMR-CNRS 5504, UMR-INRA 792, Institut National des Sciences Appliquées, Toulouse, France

Keywords
acid trehalase (Ath1p); batch culture; Fourier transform; oscillations; trehalose

Correspondence
J. François, Centre de Bioingenierie Gilbert Durand, UMR-CNRS 5504, UMR-INRA 792, Institut National des Sciences Appliquées, 135 Avenue de Rangeuil, 31077 Toulouse cedex 04, France
Fax: 00 33 5 61 559400
Tel : 00 33 5 61 559492
E-mail: fran_jm@insa-toulouse.fr
Web site: http://biopuce.insa-toulouse.fr/jmflab

(Received 15 December 2004, revised 21 January 2005, accepted 31 January 2005)

doi:10.1111/j.1742-4658.2005.04588.x

We report that autonomous oscillations, which usually happen in aerobic glucose-limited continuous cultures of yeast at low dilution rate, were also observed in trehalose discontinuous cultures of *Saccharomyces cerevisiae*. This unexpected oscillatory behaviour was therefore examined using fast Fourier transformation of online gas measurements. This robust mathematical analysis underlined the existence of two types of oscillation. The first was found to be linked to the cell cycle because (a) the periodicity corresponded to a fraction of the generation time and (b) the oscillations were accompanied by a transient increase in the budding index, mobilization of storage carbohydrates, and fermentative activity. Moreover, these oscillations occurred in a range of specific growth rates between 0.04 and 0.15 h^{-1}. All these criteria were consistent with the cell-cycle-related metabolic oscillations observed in the same range of growth rates in glucose-limited continuous cultures. The second type were short-period respiratory oscillations, independent of the specific growth rate. Both types of oscillation were found to take place consecutively and/or simultaneously during batch culture on trehalose. In addition, mobilization of intracellular trehalose emerged as a key parameter for the sustainability of these autonomous oscillations as they were no longer observed in a mutant defective in neutral trehalase activity. We propose that batch culture on trehalose may be an excellent device for further investigation of the molecular mechanisms that underlie autonomous oscillations in yeast.

Oscillatory dynamics have been extensively described in micro-organisms, in particular the yeast *Saccharomyces cerevisiae* (for recent reviews, see [1–3]). They are usually undesirable and constitute a severe limitation in industrial processes. Two types of oscillation have been reported in this yeast species. The first type are the glycolytic oscillations identified in intact yeast cells as well as in cell-free extract as transient and highly damped events after perturbation. However, sustained glycolytic oscillations have been observed in intact cells under specific conditions [4,5]. Their frequency is around 1 min in intact cells, and the synchronizing agent is thought to be acetaldehyde [2]. Oscillations of the second type are observed in glucose-limited continuous cultures of yeast, and are referred to as autonomous or 'ultradian' (i.e. cycles shorter than 24 h). These oscillations are dependent on a respiratory regimen and are classified into two groups [2]. Oscillations of the first group are related to the cell cycle. They are characterized by highly reproducible and sustained oscillations of dissolved oxygen uptake rate and CO_2 evolution rate, with periods that are dependent on the dilution rate [6]. Other metabolic parameters also oscillate in phase, such as biomass concentration, content of storage carbohydrates, and ethanol and acetate production. The molecular basis of the relationship of these oscillations to the cell cycle is still poorly understood [1,2]. In contrast, oscillations of the second group are growth rate independent. They exhibit shorter periods than the cell-cycle-related

Abbreviations
Ath1p, acid trehalase; FFT, fast Fourier transform; RQ, respiratory quotient.

oscillations and are found in yeast growing in acid conditions [7–9]. This group of oscillations also shows robust temperature and nutrient-compensation properties, i.e. their period is barely affected by variations in temperature or cell doubling rate. They have been shown to be under the control of a respiratory clock the main property of which is the time-keeping function [1,9,10].

Until now, autonomous oscillations have been described only in aerobic chemostat cultures of *S. cerevisiae* at low dilution rates. In this work, we have identified for the first time oscillatory behaviour in *S. cerevisiae* during discontinuous culture on trehalose. The purpose of this work was to examine these oscillatory patterns and compare them with those identified in continuous cultures. To this end, we exploited online gas data (O_2 and CO_2) with the fast Fourier transformation (FFT), as this algorithm has been shown to be extremely robust for analysis of autonomously oscillating yeast chemostat cultures [9,11]. Hence, we were able to identify in batch cultures on trehalose the existence of both cell-cycle-related and short-period oscillations which, contrary to previous reports in chemostat cultures [7,12], can take place consecutively and/or simultaneously. Moreover, we have shown that carbon flow and intracellular trehalose mobilization are two key parameters in the occurrence and sustainability of these autonomous oscillations under our growth conditions.

Results

Autonomous oscillations during batch culture on trehalose

With trehalose as the carbon source, the growth of the CEN.PK113-7D wild-type strain in a batch reactor started after a lag phase of ≈ 30 h with a maximal growth rate (μ_m) close to 0.07 h^{-1}. The respiratory quotient (RQ) of ≈ 1 and the absence of byproducts indicated a purely oxidative metabolism (Fig. 1A), in agreement with previous reports [13,14]. From the 65th hour to the end of the culture, the CO_2 production rate (rCO_2) exhibited oscillatory behaviour reminiscent of the oscillatory patterns described in aerobic glucose-limited continuous cultures of *S. cerevisiae* [1,6,15]. This similarity became even more striking when the rCO_2 was converted into specific CO_2 production rate (qCO_2), which is independent of the biomass concentration in the fermentor (Fig. 1C). The qCO_2 pattern was divided into two regions that showed different oscillatory properties. In region 1, the qCO_2 steadily oscillated with a period of 1.8 ± 0.1 h, around a mean value of ≈ 2 mmol·g^{-1}·h^{-1} with an amplitude of 1.1 mmol·g^{-1}·h^{-1}. In contrast, the qCO_2 signal gradually damped down over region 2 and decreased to ≈ 0.5 mmol·g^{-1}·h^{-1}, although the periodicity remained stable (0.8 ± 0.1 h). Interestingly, a transition in the oscillatory pattern could be observed

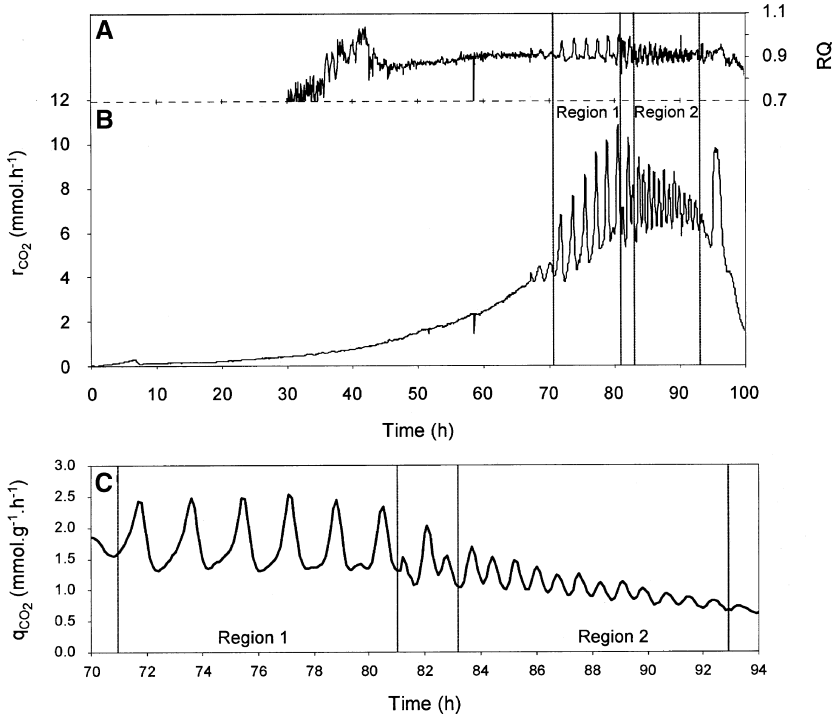

Fig. 1. Growth of CEN.PK113-7D in batch culture on trehalose. (A) RQ. (B) CO_2 production rate (rCO_2, mmol·h^{-1}). The oscillations started at ≈ 70 h (region 1) and progressively damped down to end up after 93 h of growth (region 2). (C) CO_2 specific production rate (qCO_2, mmol·g^{-1}·h^{-1}) in regions 1 and 2.

between the two regions, with the decline of one oscillation pattern and the onset of the next one with a different frequency. In summary, autonomous oscillations were identified for the first time during discontinuous, oxidative growth on trehalose, which could be split into two different types of consecutive oscillations. Furthermore, this oscillatory behaviour is probably due to the low growth rate on trehalose, which is a consequence of the low rate of trehalose hydrolysis by the periplasmic acid trehalase, Ath1p [14].

Occurrence of 'cell-cycle' and 'short-period' oscillations

The overall qCO_2 data from Fig. 1C were subjected to FFT analysis. As shown in Fig. 2A, the periodicity spectrum exhibits two maxima, one peak at 1.78 h and a doublet at $\approx$0.8 h, which may reveal the presence of two different oscillations. A refinement of the mathematical treatment of qCO_2 signal applied independently to regions 1 (71–81 h) and 2 (83–93 h) showed that the doublet corresponded to the half-period harmonic (0.84 h) of the peak at 1.76 h (Fig. 2B) and to a peak at 0.78 h (Fig. 2C), respectively. Moreover, plotting qCO_2 data from region 1 for six cycles against the same qCO_2 shifted by $\pi/2$ gave rise to a kind of limit circle, which characterizes relatively stable and well-organized oscillations (Fig. 2D). In contrast, this graphical representation of qCO_2 data from region 2 showed a damped down spiral trajectory (Fig. 2E). This behaviour was consistent with both a progressive decrease in the amplitude and a gradual decrease in the respiratory activity due to growth arrest (Fig. 1C). It is worth noting that the FFT analysis of the oxygen signal was in total agreement with those obtained with the qCO_2 analysis (Table 1). Interestingly, region 1 was characterized by a constant specific growth rate (μ) close to 0.065 h^{-1}, and the period of the oscillation could be determined as a fraction of the cell doubling time. On the other hand, the oscillation period in region 2 was barely affected by the gradual decrease in the specific growth rate (Table 1). Altogether, this mathematical analysis confirmed the existence of two types of oscillations during batch cultures on trehalose. According to the period and dependence on growth rate, one type probably corresponded to cell-cycle-related oscillations (region 1), and the other to short-term oscillations (region 2).

Cell-cycle and short-period oscillations can occur simultaneously

In a previous study, we showed that the trehalose assimilation in yeast takes place by two independent pathways. One route relies on the hydrolysis of exogenous trehalose by acid trehalase, Ath1p, localized in the periplasmic space. The second pathway requires the coupling of the trehalose uptake by a sugar transporter encoded by *AGT1* and its intracellular hydrolysis by neutral trehalase encoded by *NTH1*. We found that elimination of this second route by deletion of *AGT1* or *NTH1* resulted in mutant strain that grew

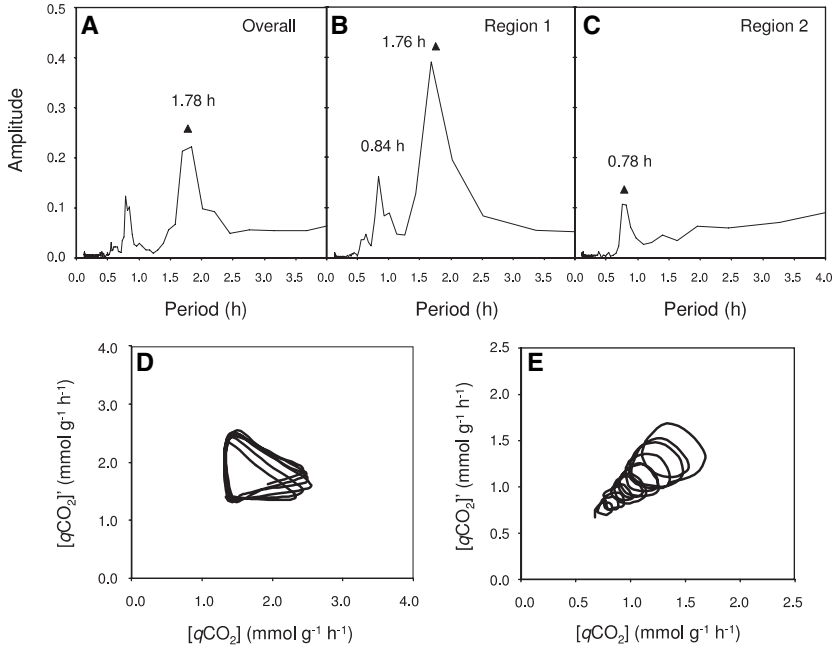

Fig. 2. Analysis of qCO_2 signal of the CEN.PK113-7D strain. (A, B and C) Power spectra from different qCO2 data sets: (A) overall data from Fig. 1C; (B) region 1; (C) data from region 2. The period values (in h) are the maxima (▲) from the Gaussian curves fitting the peaks. (D, E) Phase portrait diagrams of [qCO_2] vs. [qCO_2 advanced $\pi/2$] data obtained from regions 1 (D) and 2 (E).

Table 1. Oscillation characteristics in the wild-type and *agt1* mutant strains. Periods were calculated using FFT.

Strain	Region	Periods from qCO_2		Periods from qO_2		Specific growth rates, μ_{max} (h^{-1})	*Tg/cell cycle period
		Cell cycle	Short-term	Cell cycle	Short-term		
Wild-type	Region 1	1.76	No	1.76	No	0.065 ± 0.004	6.04
	Region 2	No	0.78	No	0.79	–[a]	–
	Overall	1.78	0.79	1.78	0.79	0.061 ± 0.008	–
agt1	Region 1	9.50	No[b]	9.45	No§	0.036 ± 0.003	2.03
	Region 2	9.28	1.15 ± 0.30	9.27	1.05 ± 0.35	0.039 ± 0.001	1.91
	Region 3	11.02	1.20 ± 0.40	11.03	1.25 ± 0.35	0.033 ± 0.004	1.89
	Overall	8.70/9.73	1.20 ± 0.40	8.70/9.65	1.20 ± 0.40	0.036 ± 0.004	2.23/2.00

[a] Specific growth rate decreasing from 0.065 to 0.055 h^{-1}. [b] Not estimated, as the signal was buried in the noise. *Tg, doubling times.

half as fast as the wild-type [14]. This finding was further illustrated in Fig. 3, which shows that the *agt1* mutant started to grow after a lag phase of ≈ 50 h and reached a maximal specific growth rate of 0.04 h^{-1}. Interestingly, autonomous oscillations could be recorded almost immediately at the start of growth, with a peak-to-peak periodicity of 10 ± 2 h (Fig. 3B). In spite of the fact that the growth was essentially oxidative, the RQ showed sudden and transient bursts over a value of 1.0, coincidentally with the peak of the

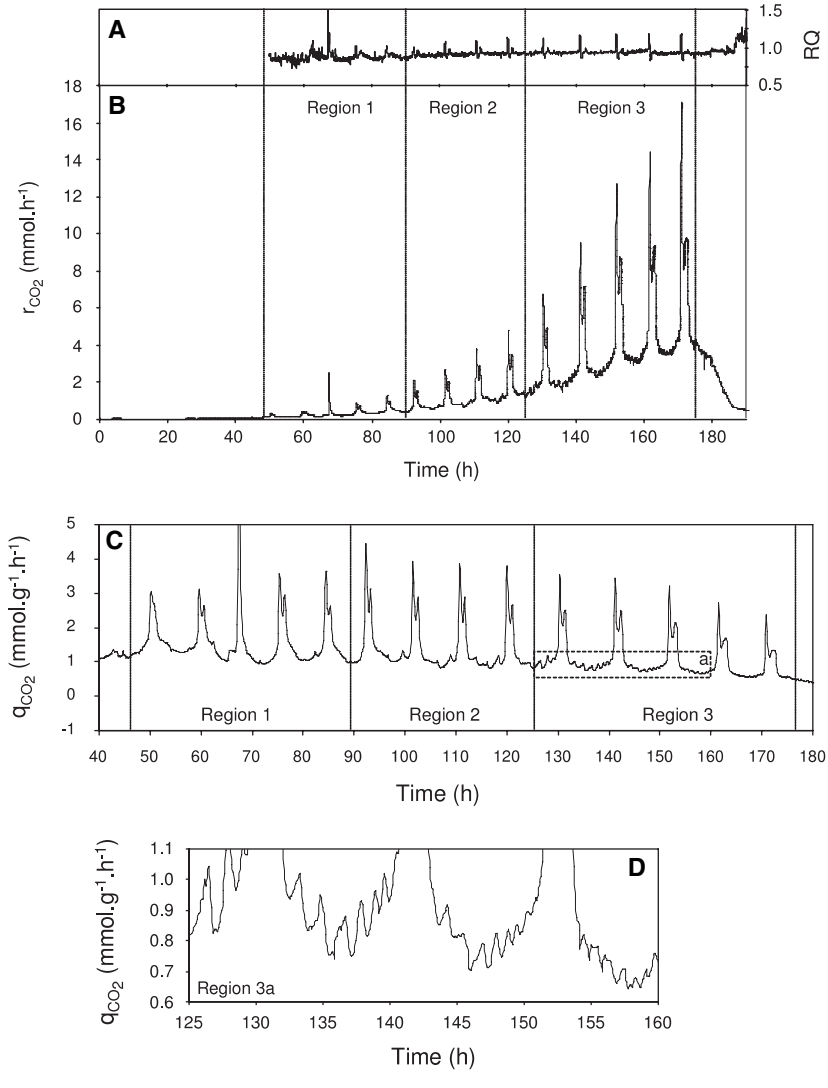

Fig. 3. Growth of the *agt1* mutant in batch culture on trehalose. (A) RQ. (B) CO_2 production rate (rCO_2, mmol·h^{-1}). The signal was partitioned into region 1 (47–89 h), region 2 (89–125 h) and region 3 (125–177 h). (C) CO_2 specific production rate (qCO_2, mmol·g^{-1}·h^{-1}) over regions 1, 2 and 3. (D) Zoom of CO_2 specific production rate (3a, delimited area from region 3).

oscillations. This transient increase in RQ indicated a weak deviation of the carbon flow to the fermentation, although concentrations of acetate or ethanol were below detection.

Conversion of rCO_2 into the specific evolution rate of CO_2 even better illustrated the oscillatory dynamics

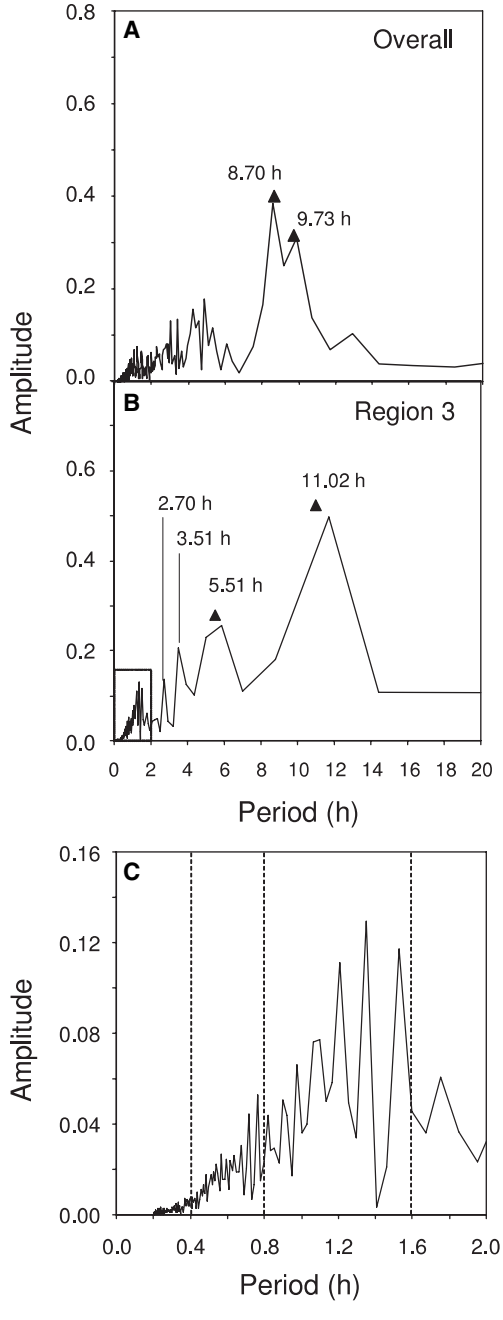

Fig. 4. Analysis of qCO_2 signal from the *agt1* mutant strain. (A, B) Power spectra of the overall $qCO2$ signal presented in Fig. 3C (A) and Fig. 3D (B). Values of the period (in h) are maxima (▲) from the Gaussian curves fitting the peaks. (C) Zoom of the power spectrum from (B) corresponding to periods below 2 h.

of the *agt1* mutant in batch culture on trehalose, which was resolved into three main regions (Fig. 3C). The qCO_2 (as well as qO_2) signal was subjected to FFT analysis. As indicated in Fig. 4A, the spectrum from overall qCO_2 data presented a doublet with two local maxima at 8.70 and 9.73 h, respectively, and a multitude of harmonics that were not well separated. This doublet could be interpreted as oscillations exhibiting two fundamental periodicities, although we rather believe that it corresponded to a transient shift in the oscillation period along the growth. When the qCO_2 signal was studied in separate nonoverlapping time windows (regions 1–3), sharp fundamental frequencies associated with the oscillation period of the signal showed up (Fig. 4B, Table 1). As an example, the spectrum from region 3 showed a parental peak (11.02 h) and its harmonics (05.51, 03.51 and 02.70 h), together with a multitude of peaks of periods below 2 h (Fig. 4B). It can be seen in Table 1 that a slight increase in the length of the oscillation period was correlated with a decrease in the specific growth rate. As a consequence, one can reasonably assume that these oscillations are related to the cell division cycle.

Region 3 (125–160 h) deserves further investigation because of the presence of an irregular oscillatory pattern composed of very short and unstable periods (Fig. 3D). As indicated in Fig. 4C, the FFT analysis of this signal gave rise to a large number of peaks ranging from 0.8 to 1.6 h and their half-period harmonics (0.4–0.8 h time window). Therefore, a fundamental periodicity of $\approx 1.20 \pm 0.4$ h (72 ± 24 min) could be estimated. This oscillation pattern was also found in region 2, but not in region 1, largely because the signal was buried in the noise (Fig. 3C; Table 1). To summarize, batch growth of the *agt1* mutant on trehalose displayed a complex oscillatory pattern that is composed of two distinct types of oscillations. As in the wild-type, we further consider that one type of oscillation is related to the cell cycle, and the other could correspond to clock-controlled ultradian respiratory oscillations [1,9].

Role of storage carbohydrate and carbon flux in oscillations

It is well established that oscillating continuous cultures of yeast at low dilution rates are characterized by periodic changes in cellular content of storage carbohydrates and budding index [15–18]. As shown in Fig. 5, similar behaviour was also found in the *agt1* mutant during batch growth on trehalose. During a typical oscillatory event (between 160 and 164 h),

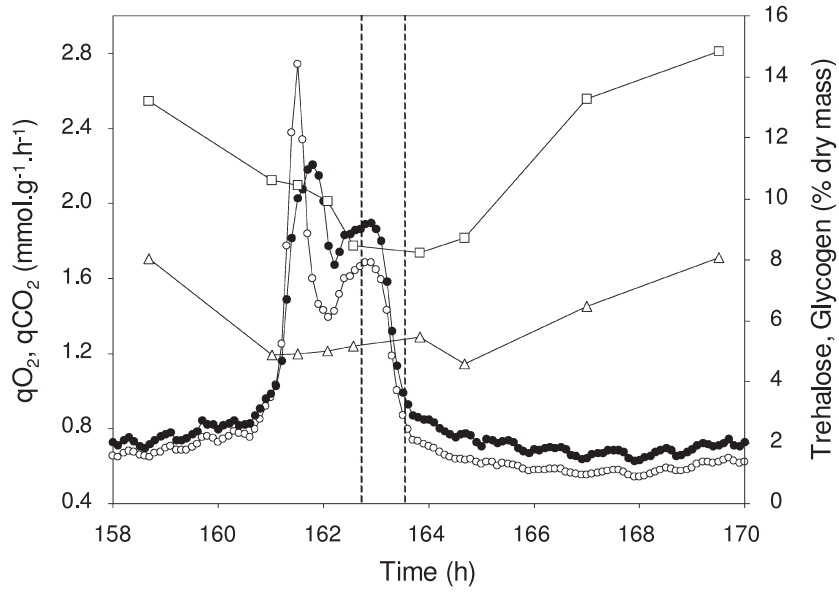

Fig. 5. Storage carbohydrate profile during one typical oscillation. Parameters were measured during one oscillation period (time window 158–170 h from Fig. 3C). Intracellular glycogen (□) and trehalose (△), qO_2 (●) and qCO_2 (○). The area between dashed lines corresponds to the burst of budding.

about 37% (of dry mass) of storage carbohydrates were mobilized, which corresponded to 2.51 mmol $C{\cdot}g^{-1}$ (dry mass), i.e. 0.85 mmol $C{\cdot}g^{-1}$ from trehalose and 1.66 mmol $C{\cdot}g^{-1}$ from glycogen. This increase in carbon flux was closely equivalent to that of the qCO_2 ($\approx$ 2.37 mmol $C{\cdot}g^{-1}$ dry mass) measured within the same time window, and thus, it could account for the transient increase in RQ during these oscillations (Fig. 3A). In addition, this transient increase was accompanied by a transient burst of budding (163–164 h) (Fig. 5).

In aerobic glucose-limited continuous cultures, the intracellular glycogen was shown to be important for both short-period [8] and cell-cycle-related oscillations [17,19], whereas the importance of trehalose was not so clear-cut. In this work, we found that these autonomous oscillations were not observed in a *nth1* mutant deficient for intracellular trehalose mobilization, whereas this mutant did show similar macrokinetic properties to those of an *agt1* mutant [14]. As cell-cycle-related oscillations have been reported to occur in a range of dilution rates of 0.03–0.15 h^{-1} [9,16,19], the specific growth rate was proposed as another critical factor for their occurrence and sustainability. Likewise, in batch cultures on trehalose, oscillatory dynamics as well as intracellular accumulation of storage carbohydrate were abolished by increasing the specific growth rate from 0.07 to 0.15 h^{-1} (data not shown). This increase in specific growth rate was achieved by overexpressing *ATH1* which encodes the periplasmic-localized acid trehalase [14]. Conversely, deletion of *ATH1* resulted in a reduction of specific growth rate on trehalose below $< 0.030\ h^{-1}$, and interestingly, this mutant no longer exhibited oscillations (data not shown).

Discussion

In this work, we show for the first time the existence of autonomous oscillations in batch cultures on trehalose. This behaviour is similar to what is observed in aerobic glucose-limited continuous cultures at low dilution rates (for reviews, see [1,2]). In a previous study [14], we have shown that the rate-limiting hydrolysis of trehalose by the periplasmic acid trehalase, Ath1p, resulted in both obligatory oxidative metabolism and weak, steady-state glucose flux into the yeast cells. This situation is therefore comparable to aerobic glucose-limited chemostat cultures in which the glucose feed rate is fixed by the dilution rate. Moreover, the oscillatory behaviour in trehalose batch culture was recorded at growth rates of 0.04–0.15 h^{-1}, which remarkably corresponds to the range of dilution rates in which autonomous oscillations have been reported in continuous cultures [9,16,19]. As reviewed by Richard [2] continuous culture of yeast cells can exhibit two types of autonomous oscillations: one type is partly related to the cell cycle, and the other, which is related to a shorter period, is clock-dependent. These two types of oscillation were also encountered in batch cultures on trehalose as discussed below.

The first type of oscillation was characterized by an oscillatory period, which was 105.6 min (01.76 h) in the wild-type and $\approx$600 min ($\approx$ 10 h) in the *agt1*

mutant strains. These values corresponded to a fraction of the cell doubling times, i.e. one-sixth in the wild-type and a half in the *agt1* mutant. This indicates that this type of oscillation was probably linked to the cell cycle [6]. Moreover, as observed in aerobic glucose-limited continuous culture [19], these oscillations triggered rapid and transient mobilization of storage carbohydrates which was accompanied by an increase in the fermentative activity. In conclusion, this type of oscillatory behaviour is consistent with the model of Strässle and coworkers [16,17] which described the integration between cell-cycle-related oscillations, storage carbohydrate mobilization, and fermentative activity.

The second type of oscillation, which was also observed in both wild-type and *agt1* mutant strains, had a shorter period that was independent of the specific growth rate. Accordingly, the period of the oscillations in the wild-type remained stable around 47 min (0.79 h), and only the amplitude decreased with the decline in μ that occurred during the growth of the *agt1* mutant. This decrease in the specific growth rate was mainly attributed to the inactivation process of the Agt1p trehalose transporter, as reported previously [14]. Taken together, these criteria are typical of short-term, so-called 'respiratory', oscillations which are coupled to an ultradian clock [9]. Murray *et al.* [9] showed that, in continuous cultures, this type of oscillation had a periodicity of 48 ± 3 min at a specific growth rate (or dilution rate) of 0.06 h^{-1}, and an unstable periodicity of 67 ± 14 min for μ below 0.05 h^{-1}. In our study, similar values were obtained with a stable period of 47 min for the wild-type (μ ≈0.065 h^{-1}) and an unstable period of 72 ± 21 min for the *agt1* mutant (μ ≈0.04 h^{-1}). Wolf *et al.* [20] developed a mathematical model that integrated the critical role of the sulfate assimilation pathway in the mechanism of short-term oscillations in chemostat cultures. It would be interesting to test whether this model can be applied to the oscillatory events that have been observed in batch growth on trehalose, and for which their transient characters reveal rather complex dynamics.

Experiments on oscillating continuous cultures led to the suggestion that cell-cycle-related and short-term oscillations cannot occur simultaneously [12,21]. In contrast with this idea, we found that both types of oscillation take place either consecutively or simultaneously during batch culture on trehalose. In the wild-type strain, these two oscillatory events were consecutive even if they overlapped for a short transition phase, at the moment when the specific growth rate fell. This fall may explain the extinction of the cell-cycle-related oscillations, as the quenching of this type of oscillation has been shown to occur in chemostat cultures by decreasing the dilution rate between two operating points [22]. Alternatively, the period of short-term oscillations is about half that of the cell cycle related oscillations, which may lead to phase interferences. This makes the coexistence of these two oscillatory events unlikely [12,21]. The coexistence of the two types of oscillation was nevertheless observed in batch growth of *agt1* mutant on trehalose, probably because their oscillation periods were very different (≈ 70 min vs. ≈600 min). Interestingly, Lloyd *et al.* [1] pointed out that short-period oscillations are only present in continuous cultures of yeast growing under acid conditions (pH < 4). Otherwise in the pH range 5.0–6.5, only autonomous cell cycle oscillations have been observed [15,19,23,24]. The fact that we observed both types of oscillation may therefore rely on an intermediate pH value, i.e. 4.75, which is the optimum pH for trehalose assimilation [14]. Although suboptimal, the growth on trehalose remains possible in a broader range of pH (4.8 ± 1.0), and it would be of interest to test whether lower or higher pH directs the oscillations towards short-term or cell-cycle types.

Mobilization of glycogen is an important parameter to sustain both cell-cycle-related [17] and short-term oscillations [8]. In this work, we observed that cell-cycle-related oscillations were accompanied by transient degradation of glycogen and trehalose. However, we found that a mutant defective in trehalose mobilization did not harbour any oscillatory behaviour during growth on trehalose, although it still accumulated glycogen. This finding not only confirmed the role of storage carbohydrates in the sustainability of cell-cycle-related oscillations, but it showed for the first time that mobilization of trehalose was indispensable to obtain this type of oscillation under our growth conditions. Early reports have related cyclic changes in reserve carbohydrates together with trehalase activity in phase with budding in chemostat cultures under glucose limitation [25,26]. More recently, a genome-wide analysis of transcript levels during the cell cycle of yeast retrieved cycling candidates, including *NTH1* and other genes in the metabolism of reserve carbohydrates (*TSL1, GSY1*, *GPH1*) [27]. Although this global study did not reveal *TPS1* (encoding trehalose-6-phosphate synthase), more recent work using continuous cultures showed oscillatory behaviour of *TPS1* that is apparently under the control of Gts1p [28]. Interestingly, this protein was reported to affect the timing of the budding and cell size of the yeast [24,29] and to stabilize short-term oscillations [30]. As proposed by these authors, it is possible that the entire metabolome is co-ordinated to produce the oscillations, and any dele-

tion of gene products associated with the central oscillating loop could theoretically be fatal [30]. This is the case with the key regulator Gts1p. Our results suggest that the neutral trehalase, and more likely other key factors from the metabolism of reserve carbohydrates, may be associated with this putative central oscillating loop.

Conclusion

In this work, we show that oscillatory dynamics are not restricted to aerobic glucose-limited continuous cultures, but can also occur in batch cultures. However, the general traits that allow the existence of autonomous oscillations seem to be identical in the two modes of cultivation. These are (a) oxidative metabolism and (b) a low glucose feeding rate. The latter is guaranteed in batch cultures on trehalose by the rate-limiting periplasmic acid trehalase-dependent hydrolysis of the disaccharide. Contrary to results obtained in continuous cultures, the two types of autonomous oscillation, namely the cell-cycle-related and short-period oscillations, can coexist in batch cultures on trehalose. Taken together, the use of this growth condition may be a useful alternative to time-consuming continuous cultures to further dissect the molecular mechanisms of autonomous oscillations in yeast cells.

Experimental procedures

Plasmid and strains

The haploid strain CEN.PK113-7D (MATa *MAL2–8^c SUC2*), a prototrophic *MAL* constitutive strain from P. Kötter (Institute of Microbiology, University of Frankfurt, Germany [31]), and its auxotrophic *ura3_52 leu2 his3* derivative were used as the wild-type and host for transformation (Table 2). The construction of the mutant strains (*agt1*, *nth1* and *ath1*) and pATH1 (*URA3* auxotrophic marker) which bears *ATH1* under *TDH1* promoter have been described [14]. The *in vitro* activity of acid trehalase was increased by 10–20-fold on transformation of the wild-type by this plasmid [14].

Table 2. Strains used in this work.

Yeast strains		Source
CEN.PK113-7D	*a MAL2-8^c SUC2*	P. Kötter [31]
CEN.PK113-1A	*α MAL2-8^c SUC2*	P. Kötter [31]
CEN.PK113-5D	*a MAL2-8^c SUC2 HIS3 LEU2 ura3–52*	P. Kötter [31]
nth1	*a MAL2-8^c SUC2 nth1Δ*::kanMX4	M. Jules [14]
agt1	*α MAL2-8^c SUC2 agt1Δ::kanMX4*	M. Jules [14]
ath1	*a MAL2-8^c SUC2 ath1Δ::kanMX4*	M. Jules [14]

Shake flask culture conditions

Yeast precultures were routinely prepared in 1-L shake flasks containing 200 mL YN synthetic medium (yeast nitrogen base without amino acids; Difco Laboratories (Sparks, MD, USA); 1.7 $g \cdot L^{-1}$; plus ammonium sulphate 5 $g \cdot L^{-1}$) containing 2% (w/v) trehalose as the carbon source, buffered at pH 4.8 by the addition of 14.3 $g \cdot L^{-1}$ succinic acid and 6 $g \cdot L^{-1}$ NaOH. Growth was followed by measuring A_{600} with an Easyspec IV spectrophotometer (Safas, Monaco, France). A_{600} values were converted into cell dry mass using a calibration curve established for the CEN.PK113-7D strain (1 A_{600} unit corresponds to 0.41 g dry cell$\cdot L^{-1}$). The maximal specific growth rate (μ_{max}) of the cultures was calculated by fitting an exponential regression over the experimental points [32]. These points were selected to yield a correlation coefficient (r^2) higher than 0.998. The μ constant from the equation $A_{600} = b\exp(\mu t)$ is the maximal specific growth rate.

Batch culture conditions

Batch cultures were performed in 2-L bioreactors (Setric Genie Industriel, Toulouse, France) with an initial working volume of 1.5 L of YN medium containing trehalose 2% (w/v) at pH 4.8 (set by the addition of pure orthophosphoric acid). The temperature was kept constant at 30 °C, and the pH of the medium was maintained at 4.8 by the addition of 2 M NaOH. The dissolved oxygen concentration was set above 20% of air saturation in the liquid phase by using a dry air flow of 10 $L \cdot h^{-1}$ and variable agitation. Growth was monitored independently by gas analysis, A_{600}, and cell dry mass. After correlating A_{600} with cell dry mass, biomass (X, $g \cdot L^{-1}$) was used to calculate the growth rate (dX/dt, r_x, $g \cdot L^{-1} \cdot h^{-1}$) as well as the specific growth rate ($1/X \times dX/dt$, μ, h^{-1}). The average specific growth rate (μ_a, h^{-1}) is defined as an average of μ data on the targeted time window and is given with its expected standard deviation.

Determination of trehalose, glycogen and extracellular metabolites

Samples (2 mL) were quickly harvested from the fermentor using a syringe, quickly transferred to Eppendorf tubes, and centrifuged for 2 min at 4000 ***g***. The pellet was used for glycogen and trehalose determination as described previously [33]. Storage carbohydrates were expressed as percentage of dry mass (g storage carbohydrate per g dry biomass) or mmol $C \cdot g^{-1}$ (mmol carbon per g dry biomass). Extracellular trehalose, glucose, acetic acid, ethanol and other byproducts were measured in the cell-free supernatant by HPLC using an Aminex® HPX-87H column (Bio-Rad Laboratories). The column was

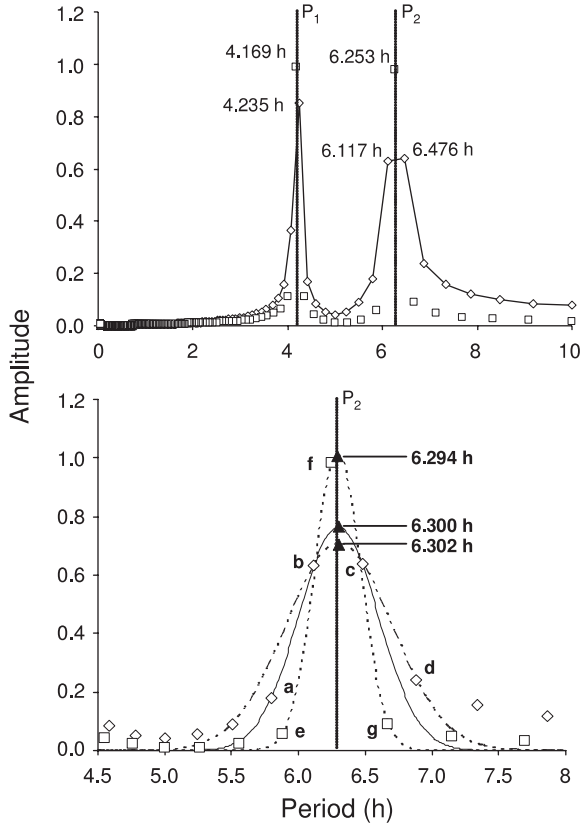

Fig. 6. Power spectrum of the equation $y = \sin(3x/2) + \sin x$. (A) FFT of two discrete data sets, the first with 1000 points (□) and the second with 2000 points (◇), over a 100 h time window. Vertical lines cross the *x*-axis at the theoretical periods of the two sinusoids from the equation $P_1 = 3\pi/2$ (4.189 h) and $P_2 = 2\pi$ (6.283 h). Other values on the figure (expressed in h) are those obtained from FFT of the equation. (B) The values of the periods (in hours) are the maxima (▲) of the Gaussian fitting curves drawn from points a, b, c (◇, plain line); b, c, d (◇, dashed line) or e, f, g (□, dashed line).

eluted at 48 °C with 5 mM H_2SO_4 at a flow rate of 0.5 mL·min^{-1}. Concentrations of these compounds were determined by using a Waters model 410 refractive index detector.

Other analytical procedures

Online estimation of O_2, CO_2, and N_2 molar fractions of inlet and exhaust gases was performed by MS (PRIMA 600S; VG gas, Manchester, UK) with a relative accuracy of 0.1%. Rates of gas consumption or production (rO_2 and rCO_2 in mmol·h^{-1}) were used for the calculation of the respiratory quotient (RQ, where $RQ = rO_2/rCO_2$). Specific rates of gas consumption or production (qO_2 and qCO_2 in mmol·g^{-1}·h^{-1}) were used for oscillatory dynamic analysis and periodicity determination.

Computational methods

Analysis of biological oscillatory dynamics were performed using FFT, a robust method used to characterize the frequency spectrum of the underlying process [11]. Exhaust gaseous data (i.e. qCO_2) were treated with XNUMBERS.XLA software (version 3.0, October 2003), which is an Excel add-in (xla) consisting of a set of hundreds of mathematical functions. Among these, the DFSP function corresponds to the so-called 'Fourier spectrum' which leads to the periodicity (1/frequency) of the oscillatory phenomenon.

As biological data are not continuous but discrete, the FFT analysis usually leads to an under-sampled distribution through the period axis and therefore to an approximate periodicity determination. A better estimation of the periodicity can be obtained by fitting on this FFT distribution a Gaussian curve with weighting to centralized points using the following equation:

$$y = y_0 e^{-\frac{(x-\mu)^2}{2\sigma^2}}$$

where, x is the period, μ the 'mean' or period of the phenomenon under investigation, σ^2 the variance, y the amplitude, and y_0 the amplitude of the mean. As an example, Fig. 6 shows the FFT analysis of an oscillatory phenomenon, which is the sum of two sine functions [$y = \sin(3x/2) + \sin x$] the theoretical periods of which are $P_1 = 3\pi/2$ (4.189 h) and $P_2 = 2\pi$ (6.283 h), respectively (vertical lines, Fig. 6A). Two peaks can be visualized on the graph, one at ≈4.215 h corresponding to the period of $\sin(3x/2)$, and the second between 6.117 and 6.476 h and corresponding to the period of $\sin x$. For the second peak (Fig. 6B), any Gaussian estimation of the peak's maximum approximates the theoretical period P_2 (2π). Therefore, this method applied to the above equation reduces the period's error to 1%. When applied to our biological data, this method led to an accuracy for the periodicity of > 95%. To examine the stability of oscillations, we embedded the time series (qCO_2 and qO_2) data in a two-dimensional space: $[qCO_2]'$ (= qCO_2 data advanced $\pi/2$) vs. $[qCO_2]$. This will align as a closed trajectory if the data have periodicity [24,30,34] (Fig. 2D).

Acknowledgements

This work was supported in part by the Microbiology and Pathogenicity program of the French Ministry of Education. M.J. was supported by a doctoral grant from the French Ministry of Education and Research. We also thank Lutz Brush and Sergei Sokol for their help with the fast Fourier transform.

References

1 Lloyd D, Lemar KM, Salgado EJ, Gould TM & Murray DB (2003) Respiratory oscillations in yeast:

mitochondrial reactive oxygen species, apoptosis and time; a hypothesis. *FEMS Yeast Res* **3**, 333–339.
2 Richard P (2003) The rhythm of yeast. *FEMS Microbiol Rev* **27**, 547–557.
3 Patnaik PR (2003) Oscillatory metabolism of *Saccharomyces cerevisiae*: an overview of mechanisms and models. *Biotechnol Adv* **21**, 183–192.
4 Dano S, Sorensen PG & Hynne F (1999) Sustained oscillations in living cells. *Nature* **402**, 320–322.
5 Poulsen AK, Lauritsen FR & Folke Olsen L (2004) Sustained glycolytic oscillations: no need for cyanide. *FEMS Microbiol Lett* **236**, 261–266.
6 Beuse M, Bartling R, Kopmann A, Diekmann H & Thoma M (1998) Effect of the dilution rate on the mode of oscillation in continuous cultures of *Saccharomyces cerevisiae*. *J Biotechnol* **61**, 15–31.
7 Keulers M, Satroutdinov AD, Suzuki T & Kuriyama H (1996) Synchronization affector of autonomous short-period-sustained oscillation of *Saccharomyces cerevisiae*. *Yeast* **12**, 673–682.
8 Satroutdinov AD, Kuriyama H & Kobayashi H (1992) Oscillatory metabolism of *Saccharomyces cerevisiae* in continuous culture. *FEMS Microbiol Lett* **77**, 261–267.
9 Murray DB, Roller S, Kuriyama H & Lloyd D (2001) Clock control of ultradian respiratory oscillation found during yeast continuous culture. *J Bacteriol* **183**, 7253–7259.
10 Lloyd D (2003) Effects of uncoupling of mitochondrial energy conservation on the ultradian clock-driven oscillations in *Saccharomyces cerevisiae* continuous culture. *Mitochondrion* **3**, 139–146.
11 Birol G, Zamamiri AQ & Hjortso A (2000) Frequency analysis of autonomously oscillating yeast cultures. *Process Biochem* **35**, 1085–1091.
12 Beuse M, Kopmann A, Diekmann H & Thoma M (1999) Oxygen, pH values, and carbon source induced changes of the mode of oscillation in Synchronous continuous culture of *Saccharomyces cerevisiae*. *Biotechnol Bioeng* **63**, 410–417.
13 Malluta EF, Decker P & Stambuk BU (2000) The Kluyver effect for trehalose in *Saccharomyces cerevisiae*. *J Basic Microbiol* **40**, 199–205.
14 Jules M, Guillou V, Francois J & Parrou JL (2004) Two distinct pathways for trehalose assimilation in the yeast *Saccharomyces cerevisiae*. *Appl Environ Microbiol* **70**, 2771–2778.
15 Duboc P, Marison I & von Stockar U (1996) Physiology of *Saccharomyces cerevisiae* during cell cycle oscillations. *J Biotechnol* **51**, 57–72.
16 Strässle C, Sonnleitner B & Fiechter A (1989) A predictive model for the spontaneous synchronization of *Saccharomyces cerevisiae* grown in continuous culture. II. Experimental verification. *J Biotechnol* **9**, 191–208.
17 Strässle C, Sonnleitner B & Fiechter A (1988) A predictive model for the spontaneous synchronization of *Saccharomyces cerevisiae* grown in continuous culture. I. Concept. *J Biotechnol* **7**, 299–317.
18 Müller D, Exler S, Aguilera-Vázquez L, Guerrero-Martín S & Reuss M (2003) Cyclic AMP mediates the cell cycle dynamics of energy metabolism in *Saccharomyces cerevisiae*. *Yeast* **20**, 351–367.
19 Munch T, Sonnleitner B & Fiechter A (1992) The decisive role of the *Saccharomyces cerevisiae* cell cycle behaviour for dynamic growth characterization. *J Biotechnol* **22**, 329–351.
20 Wolf J, Sohn HY, Heinrich R & Kuriyama H (2001) Mathematical analysis of a mechanism for autonomous metabolic oscillations in continuous culture of *Saccharomyces cerevisiae*. *FEBS Lett* **499**, 230–234.
21 Keulers M, Suzuki T, Satroutdinov AD & Kuriyama H (1996) Autonomous metabolic oscillation in continuous culture of *Saccharomyces cerevisiae* grown on ethanol. *FEMS Microbiol Lett* **142**, 253–258.
22 Zamamiri AQ, Birol G & Hjortso A (2001) Multiple stable states and hysteresis in continuous, oscillating cultures of budding yeast. *Biotechnol Bioeng* **75**, 305–312.
23 Schena M, Freedman LP & Yamamoto KR (1989) Mutations in the glucocorticoid receptor zinc finger region that distinguish interdigitated DNA binding and transcriptional enhancement activities. *Genes Dev* **3**, 1590–1601.
24 Akiyama S & Tsurugi K (2003) The *GTS1* gene product facilitates the self-organization of the energy metabolism oscillation in the continuous culture of the yeast *Saccharomyces cerevisiae*. *FEMS Microbiol Lett* **228**, 105–110.
25 Kuenzi MT & Fiechter A (1969) Changes in carbohydrate composition and trehalase-activity during the budding cycle of *Saccharomyces cerevisiae*. *Arch Microbiol* **64**, 396–407.
26 Van Doorn J, Scholte ME, Postma PW, Van Driel R & van Dam K (1988) Regulation of trehalase activity during the cell cycle of *Saccharomyces cerevisiae*. *J Gen Microbiol* **134**, 785–790.
27 Spellman PT, Sherlock G, Zhang MQ, Iyer VR, Anders K, Eisen MB, Brown PO, Botstein D & Futcher B (1998) Comprehensive identification of cell cycle-regulated genes of the yeast *Saccharomyces cerevisiae* by microarray hybridization. *Mol Biol Cell* **9**, 3273–3297.
28 Xu Z, Yaguchi S & Tsurugi K (2004) Gts1p stabilizes oscillations in energy metabolism by activating the transcription of *TPS1* encoding trehalose-6-phosphate synthase 1 in the yeast *Saccharomyces cerevisiae*. *Biochem J* **383**, 171–178.
29 Mitsui K, Yaguchi S & Tsurugi K (1994) The *GTS1* gene, which contains a Gly-Thr repeat, affects the timing of budding and cell size of the yeast *Saccharomyces cerevisiae*. *Mol Cell Biol* **14**, 5569–5578.

30 Adams CA, Kuriyama H, Lloyd D & Murray DB (2003) The Gts1 protein stabilizes the autonomous oscillator in yeast. *Yeast* **20**, 463–470.
31 van Dijken JP, Bauer J, Brambilla L, Duboc P, Francois JM, Gancedo C, Giuseppin ML, Heijnen JJ, Hoare M, Lange HC *et al*. (2000) An interlaboratory comparison of physiological and genetic properties of four *Saccharomyces cerevisiae* strains. *Enzyme Microb Technol* **26**, 706–714.
32 Parrou JL, Enjalbert B, Plourde L, Bauche A, Gonzalez B & François J (1999) Dynamic responses of reserve carbohydrate metabolism under carbon and nitrogen limitations in *Saccharomyces cerevisiae*. *Yeast* **15**, 191–203.
33 Parrou JL & François J (1997) A simplified procedure for a rapid and reliable assay of both glycogen and trehalose in whole yeast cells. *Anal Biochem* **248**, 186–188.
34 Hans MA, Heinzle E & Wittmann C (2003) Free intracellular amino acid pools during autonomous oscillations in *Saccharomyces cerevisiae*. *Biotechnol Bioeng* **82**, 143–151.